Earth and Planetary Science Letters 301 (2011) 285–296

Contents lists available at ScienceDirect

Earth and Planetary Science Letters

journal homepage: www.elsevier.com/locate/epsl

Empirical relationship between leaf wax *n*-alkane δD and altitude in the Wuyi, Shennongjia and Tianshan Mountains, China: Implications for paleoaltimetry

Pan Luo [a,*], Ping'an Peng [b], Gerd Gleixner [c], Zhuo Zheng [d], Zhonghe Pang [a], Zhongli Ding [a]

[a] Key Laboratory of Cenozoic Geology and Environment, Institute of Geology and Geophysics, Chinese Academy of Sciences, Beijing 100029, China
[b] Guangzhou Institute of Geochemistry, Chinese Academy of Sciences, Guangzhou 510640, China
[c] Max Planck Institute for Biogeochemistry, Jena 07745, Germany
[d] Department of Earth Sciences, Sun Yat-sen University, Guangzhou 510275, China

ARTICLE INFO

Article history:
Received 1 August 2010
Received in revised form 27 October 2010
Accepted 7 November 2010
Available online 3 December 2010

Editor: P. DeMenocal

Keywords:
leaf wax
n-alkane
deuterium/hydrogen isotopic ratio
inverse altitude effect
paleoelevation
paleoaltimetry

ABSTRACT

Estimating past elevation not only provides evidence for vertical movements of the Earth's lithosphere, but also increases our understanding of interactions between tectonics, relief and climate in geological history. Development of biomarker hydrogen isotope-based paleoaltimetry techniques that can be applied to a wide range of sample types is therefore of continuing importance. Here we present leaf wax-derived *n*-alkane δD (δD_{wax}) values along three soil altitudinal transects, at different latitudes, in the Wuyi, Shennongjia and Tianshan Mountains in China, to investigate δD_{wax} gradients and the apparent fractionation between leaf wax and precipitation ($\varepsilon_{wax\text{-}p}$).

We find that soil δD_{wax} track altitudinal variations of precipitation δD along the three transects that span variable environment conditions and vertical vegetation spectra. An empirical δD_{wax}-altitude relation is therefore established in which the average δD_{wax} lapse rate of -2.27 ± 0.38‰/100 m is suitable for predicting relative paleoelevation change (relative uplift). The application of this empirical gradient is restricted to phases in the mountain uplift stage when the atmospheric circulation had not distinctly changed and to when the climate was not arid. An empirical δD_{wax}–latitude–altitude formula is also calculated: $\delta D_{wax} = 3.483LAT - 0.0227ALT - 261.5$, which gives the preliminary spatial distribution pattern of δD_{wax} in modern China.

Mean value of $\varepsilon_{wax\text{-}p}$ in the extreme humid Wuyi Mountains is quite negative (−154‰), compared to the humid Shennongjia (−129‰) and the arid (but with abundant summer precipitation) Tianshan Mountains (−130‰), which suggests aridity or water availability in the growing season is the primary factor controlling soil/sediment $\varepsilon_{wax\text{-}p}$. Along the Tianshan transects, values of $\varepsilon_{wax\text{-}p}$ are speculated to be constant with altitude; while along the Wuyi and Shennongjia transects, $\varepsilon_{wax\text{-}p}$ are also constant at the low-mid altitudes, but become slightly more negative at high altitudes which could be attributed to overestimates of precipitation δD or the vegetation shift to grass/conifer.

Additionally, a reversal of altitude effect in the vertical variation of δD_{wax} was found in the alpine zone of the Tianshan Mountains, which might be caused by atmospheric circulation change with altitude. This implies that the paleo-circulation pattern and its changes should also be evaluated when stable isotope-based paleoaltimetry is applied.

1. Introduction

Defining and quantifying vertical movements of the Earth's lithosphere is a common and fundamental activity for geoscientists, where paleoelevation can be used to measure, indicate or constrain the changes in a geophysical property or process (Teixell et al., 2009). In particular, for orogenic belts, elevation changes of the Earth's surface are one of the most informative measures of continental deformation. The elevation history offers a tool for understanding the driving forces of deformation, and provides insights into how strain is vertically partitioned and how mass is redistributed or conserved in the lithosphere (Clark, 2007). Additionally, paleoelevation is also an important variable in the evolution of landscape (Bishop, 2007) and climate (Kutzbach et al., 1989). Therefore, quantitative estimates of paleoelevation would improve our understanding of tectonic-relief-climate interactions (Molnar et al., 2010; Ruddiman et al., 1997).

Stable isotope-based paleoaltimetry has been a useful quantitative method for estimating the paleoelevation of mountains and plateaus, and has been extensively applied in the Tibet, the Andes, the Sierra Nevada and elsewhere (Rowley and Garzione, 2007, and references

* Corresponding author. Tel.: +86 10 82998378; fax: +86 10 62010846.
E-mail addresses: luopan@mail.iggcas.ac.cn, ipanluo@gmail.com (P. Luo).

0012-821X/$ – see front matter © 2010 Elsevier B.V. All rights reserved.
doi:10.1016/j.epsl.2010.11.012

therein). The principle behind this approach is the isotopic altitude effect in atmospheric moisture, rain, snow, as has been established by numerous observations (e.g., Ambach et al., 1968; Araguás-Araguás et al., 2000; Gonfiantini et al., 2001; Poage and Chamberlain, 2001). When air masses are orographically uplifted, they cool and preferentially precipitate moisture with the heavier isotopes of oxygen and hydrogen, thus $\delta^{18}O$ and δD values of precipitation become more negative as altitude increases. Therefore, if the isotopic composition of water at a particular location in geological time is determined, the paleoaltitude can be estimated via empirical (e.g., Garzione et al., 2000) or theoretical (e.g., Rowley et al., 2001) relations between the isotopic composition of precipitation and altitude. Previous studies have focused on authigenic or pedogenic minerals which preserve isotopic composition of ancient water, but the fidelity is affected by evaporation, temperature of formation, and post-depositional isotope exchange (Blisniuk and Stern, 2005; Mulch and Chamberlain, 2007; Quade et al., 2007). Each paleoaltimetric approach, for example flora fossils (Forest, 2007; Meyer, 2007) and vesicular basalts (Sahagian and Proussevitch, 2007), has its own inherent strengths and weaknesses, therefore combined estimates based upon independent techniques are desired, especially when these above-mentioned paleoelevation markers are absent. Development of paleoaltimetry that can be applied to a wide range of sample types is therefore of continuing importance.

In modern vascular plants, the δD values of *n*-alkanes derived from leaf waxes reflect the δD of water used by the plants (Bi et al., 2005; Chikaraishi and Naraoka, 2003; Sachse et al., 2006). Further, δD values of leaf wax-derived *n*-alkanes preserved in sediments (Hou et al., 2008; Sachse et al., 2004) and soils (Rao et al., 2009) spanning a large range of environmental conditions and vegetations carry isochronous changes with δD values of precipitation. Moreover, among the variable biochemicals of leaf wax, *n*-alkanes are the most abundant and the least reactive component among the constituents of ancient sedimentary organic matter, and the carbon-bound hydrogen of *n*-alkanes do not readily exchange with ambient water at low temperatures (Schimmelmann et al., 2006; Sessions et al., 2004; Yang and Huang, 2003). Hence, ancient *n*-alkane δD provides an approach to reconstruct the δD of paleoprecipitation, and finally paleoelevation. A soil *n*-alkane δD altitudinal gradient along Mount Gongga, China has confirmed the potential of leaf wax-derived *n*-alkane δD as a proxy for altitude (Jia et al., 2008) and this new biomarker isotope-based paleoaltimetry technique has been applied to the Cenozoic Tibetan Plateau (Polissar et al., 2009) and the Sierra Nevada (Hren et al., 2010).

Previous studies have shown that δD of precipitation plays a fundamental control on leaf wax δD values (Liu and Yang, 2008, and references therein). However, there exists an apparent (net) fractionation between leaf wax and precipitation ($\varepsilon_{wax\text{-}p}$), which is determined by the D-enrichment of ecosystem evapotranspiration (soil evaporation and plant transpiration) and D-depletion of biosynthesis. $\varepsilon_{wax\text{-}p}$ is not constant, and can be altered by two prominent factors: (1) changes in evaporative isotopic enrichment at different environmental parameters, e.g., RH (relative humidity) or P/E (precipitation/evaporation), due to evaporation from soil and leaf surfaces (Sachse et al., 2004, 2006; Smith and Freeman, 2006), and (2) variable isotopic discriminations among plant types due to different physiological characteristics related to water use, including plant type (e.g., tree/shrub/grass or angiosperm vs. conifer), photosynthetic pathway (C3 vs. C4), leaf anatomy/morphology (stomata / interveinal distance), and water use strategy of roots (deep-rooted vs. shallow-rooted) (Chikaraishi and Naraoka, 2003; Hou et al., 2007a,b; Krull et al., 2006; Liu et al., 2006; Pedentchouk et al., 2008; Sachse et al., 2006; Smith and Freeman, 2006). These factors are intricate and interacting, e.g., climate change usually causes changes in vegetation and the adaptation of plant physiology. Taxon-specific $\varepsilon_{wax\text{-}p}$, in terms of vegetation type, relative abundance of dominant species, the contributions of different plant types to organic matters, etc., have been suggested for use in paleoprecipitation δD reconstruction (Liu and Yang, 2008; Pedentchouk et al., 2008). However, there are at least three difficulties associated with the use of taxon-specific $\varepsilon_{wax\text{-}p}$: (1) seasonal variations in leaf wax δD (even the difference between *n*-alkanes from the same plant species) (Sachse et al., 2009; Sessions, 2006), (2) reconstructing such elaborate paleoflora and (3) separating climatic and biological effects. Therefore, estimation of past $\varepsilon_{wax\text{-}p}$ for sedimentary/paleosol leaf waxes derived from variable plants is still a challenge.

The altitudinal transect, to some extent, underpins the general pattern of climate, vegetation and landform evolution during orogenic uplift, e.g., fall in air temperature, formation or intensification of orographic rain, change in vegetation from warm to cold species, and development of glaciers (Körner, 2007; Zhang et al., 2009). Therefore, vertical nature spectra along the altitudinal transect provide the nearest living relatives fitting different stages of mountain uplift. The *n*-alkane δD-altitude relationships and $\varepsilon_{wax\text{-}p}$ based on modern altitudinal transect, which integrates climatic and biological effects, would be more close to the realistic situation during mountain uplift. However, due to the varying patterns of mountain uplift and different responses of climate, vegetation and landforms, the temporal evolution and the spatial change cannot be matched monotonously or bijectively. Therefore, more altitudinal transects are required to investigate how "regional environment" and "altitude" control $\varepsilon_{wax\text{-}p}$, and for establishing empirical *n*-alkane δD-altitude relationships.

Here, we present δD values of individual *n*-alkanes from surface soil along three altitudinal transects in the Wuyi, Shennongjia and Tianshan Mountains in China, to investigate altitudinal gradients of leaf wax-derived *n*-alkane δD. These transects are situated in very different physiographic regions (climate, vegetation, water isotope, and atmospheric circulation) that cross various vegetation (forest-meadow-cushion) and hydrological vertical zones, therefore permitting examination of the empirical relationship between *n*-alkanes δD and altitude, discussion of the variation of $\varepsilon_{wax\text{-}p}$ as "altitude" and "environment" change, and analysis of the effects of topography, climate and vegetation.

2. Study area, sampling and experiments

2.1. Altitudinal transects

The Wuyi Mountains, with the highest peak Mount Huanggang at 2158 m above sea level (m), are located in southeast China. The mountains have a mean elevation of 1100 m., and extend with a northeast–southwest direction parallel to the coast (Fig. 1). The regional warm, humid subtropical climate shows monsoon patterns and year-round precipitation. The hot season (April to September) has the greatest precipitation (Table S1), being dominated by the summer monsoon and sometimes intensified by typhoons (tropical cyclones). In the pre-monsoon months, the climate becomes relatively cold and dry. Annual mean precipitation is greater than evaporation, resulting in a positive water balance. Mean annual precipitation increases and air temperature decreases with altitude, while mean annual RH is fairly stable at 80%. Accordingly, there is a prominent change in vegetation with altitude, leading to vertical vegetation zonations (Fig. 2).

The Shennongjia Mountains, with the highest peak Shennongding (3105.4 m), lie east-west in the eastern extension of the Daba Mountains in central China. Their mean elevation is 1600 m. The mountains are situated in the transitional region between the eastern plains and the foothills of mountainous central China, and in the transitional zone from a northern subtropical to temperate climate. Mean annual temperature and precipitation of the Shennongjia Mountains are both relatively lower than those of the Wuyi Mountains, but the region is similarly characterized by a subtropical monsoon climate with a wet warm summer and cold dry winter (Table S1). The montane climate is also impacted by altitude change. With increasing altitude, mean annual air temperature decreases,

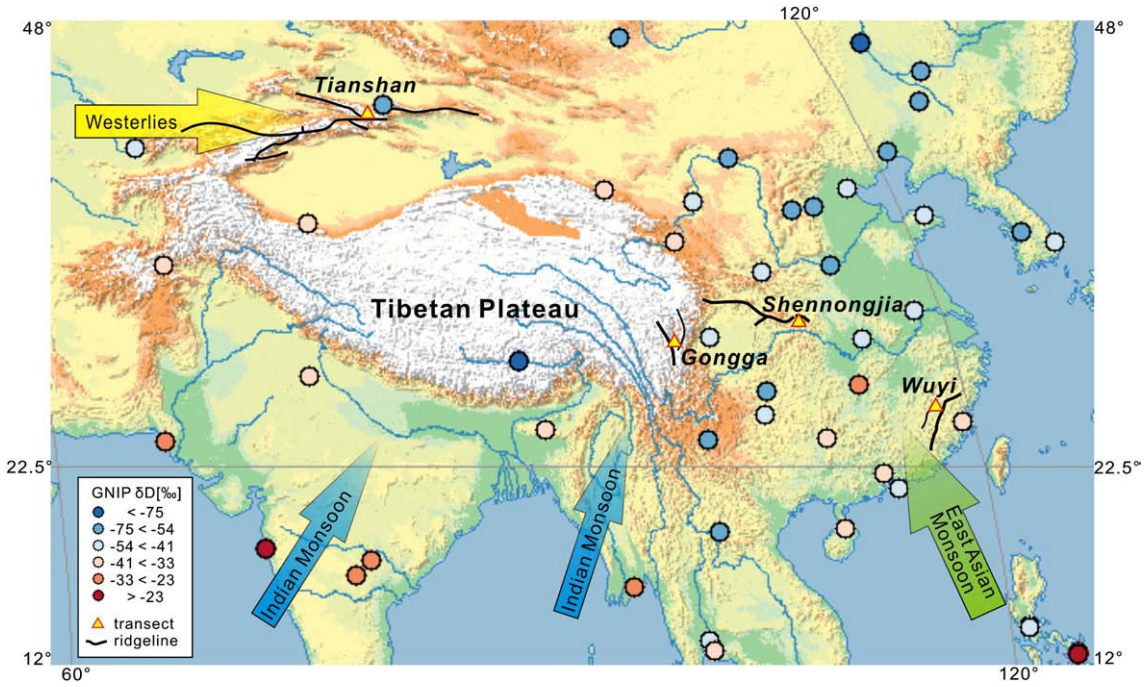

Fig. 1. Locations of soil altitudinal transects Wuyi, Shennongjia, Tianshan and Gongga (studied previously by Jia et al. (2008) on physiographic map. Ridgelines (Black curves) in study area indicate the sampling slope of transects (▲). IAEA-GNIP (Global Network of Isotopes in Precipitation) sites (●) and mean annual δD of precipitation (value ranges indicated in different colors) are projected by WISER (Water Isotope System for Data Analysis, http://nds121.iaea.org/wiser/). Dominant circulation systems (arrows) in summer show main patterns of moisture transport.

mean annual precipitation increases, and mean annual RH decreases slightly, resulting in clear vertical zones of vegetation type (Fig. 2).

The Tianshan (Tien Shan) Mountains cover a vast area, extending more than 2500 km east-west with a width of 250–350 km, thus forming a major mountain belt across Central Asia. The average elevation of the ridgeline is ~4000 m. The northern slope of the Chinese Tianshan (the Urumqi River watershed) in Xinjiang Autonomous Area, with high point Tianger II (4486 m), is selected as the altitudinal

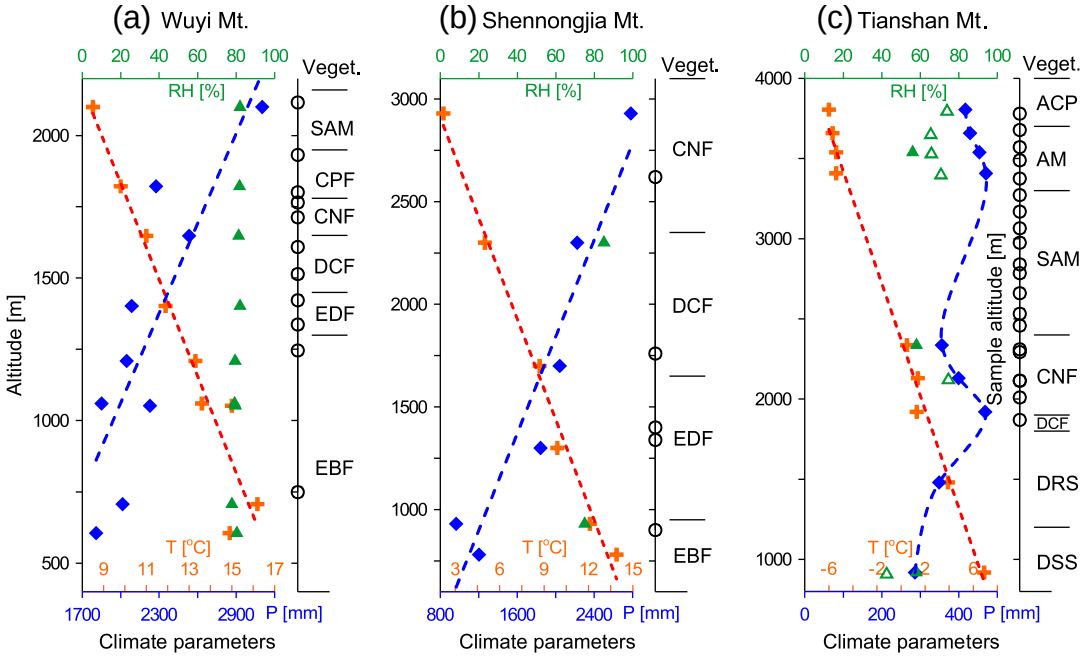

Fig. 2. Climate parameters including mean annual air temperature (+), mean annual precipitation amount (•), relative humidity (mean annual ▲, mean summer △), vertical vegetation zones and altitude distribution of sampling sites (○) along transects. Climate data of Wuyi Mt. are from meteorological observation in 1959–1960 (Zhang and Lin, 1985); for Shennongjia Mt., data from Li and Manfred (2002); for Tianshan Mt. (the Urumqi River catchment), data summarized from Annual Report of Tianshan Glaciological Station, CAS (1999–2006) and Han et al. (2004). The vertical vegetation zones of Wuyi Mt. change as increasing altitude from evergreen broad-leaved forest (abbreviated as EBF), evergreen and deciduous mixed forest (EDF), deciduous and coniferous mixed forest (DCF), coniferous forest (CNF), coppice forest (CPF) to sub-alpine meadow (SAM); for Shengnongjia Mt., from EBF, EDF, DCF to CNF; for Tianshan Mt., from desert steppe (DSS), dry steppe (DRS), DCF, CNF (characterized by homogeneous *Picea* forest and mosaic-patched meadow), SAM, alpine meadow (AM) to alpine cushion plant (ACP). Main plant types and floras in every vegetation zone are listed in Table.S2.

transect. There are 124 modern glaciers in the alpine zone and the average snowline is at ~3780 m. At the head of Urumqi River (>3400 m), seven well-developed glaciers cover 20% of the source catchment area of this river. As the hinterland of Eurasia, the climate of the Tianshan area is an arid continental climate with precipitation concentrated in summer (Table S1). The main factor determining the climatic regime is the interaction between the southwestern branch of the Siberian anticyclonic circulation and cyclonic activity from the west (Aizen et al., 1997). Moisture is mainly brought by westerlies, but partly by polar air masses (Tian et al., 2007). The Tianshan Mountains are surrounded by vast desert areas: the Taklimakan Desert to the south, the Gurbantunggut Desert to the north, and the Gobi Desert to the east. The east–west orientation of the Tianshan Mountains acts as a channel for moist westerlies, and as a barrier to air masses moving from the west and north into central Asia. The Tianshan Mountains thus form a "wet island" controlling the regional climate and ecosystem.

The climatic gradient along the Tianshan transect shows decreasing mean annual air temperature with increasing altitude. Mean annual precipitation away from the mountains is less than that in montane areas. Precipitation (summer and annual) peaks in two zones: in a gap in the mountains at Yingxiongqiao (~1900 m), and in a glaciated area at Daxigou (~3500 m) (Han et al., 2004; Wang and Zhang, 1985; and see Fig. 2). As a result of this hydrological-thermal configuration, climate gradient and vertical vegetation zones along Tianshan transect are distinctly different from those of Wuyi and Shennongjia (Fig. 2).

2.2. Sampling

Surface soil samples from the Wuyi, Shennongjia and Tianshan Mountains were collected in August 2004, July 2006 and August 2008, respectively. In the Wuyi Mountains, one or two samples were taken from every vegetation zone along the northwest slope. Despite the east slope facing windwards during typhoons, monsoons travel in the same north–south direction as the strike of the range. The combination of this layout with the relatively low average elevation and high precipitation over this area leads to no significant differences in precipitation with slope aspect (Zhang and Lin, 1985). Sampling sites in the Shennongjia Mountains were situated on the eastern and southern slopes, both of which are windward to the summer monsoon and have higher precipitation than the leeward slopes (Li and Manfred, 2002). Samples from the Tianshan Mountains were collected at ~100 m altitude intervals, along the northern slope of the Urumqi River valley, where precipitation is distinctly higher than on the southern slope (Han et al., 2004). We did not sample soils from the desert steppe and dry steppe in the lower areas of the Tianshan Mountains because of sparse cover and intensive agricultural and pastoral influences.

All sample sites were located on slopes far away from rivers and surface water bodies. The altitude of each site was determined using a handheld GPS unit with an error of ±10 m. At each site, three samples of the A horizon (0–5 cm) were collected (after removal of the litter layer) with a small metal scoop, at random from within a ~5 m radius under the representative plant(s) of the general vegetation. Samples were wrapped with aluminum foil and sealed on site in a polyethylene zipper bag.

2.3. Sample analysis

2.3.1. Sample preparation

Soil samples were firstly ground and freeze-dried. Soluble organic matter was extracted using a Soxhlet extractor with a dichloromethane/methanol mixture (v:v = 93:7) for 72 hours. The total extract was separated using a column with 5% H_2O-deactivated silica gel-alumina, and the aliphatic fraction was eluted by hexane for gas chromatography (GC) analysis. Then, the aliphatic fraction was further purified by urea adduction for measurement of compound-specific hydrogen isotope composition.

2.3.2. Gas chromatography

n-Alkanes of the aliphatic fraction were identified and quantified using a Hewlett–Packard 6890 gas chromatograph with flame ionization detector (FID). The injector temperature was maintained at 290 °C, with a detector temperature of 300 °C. The GC temperature program increased from 70 to 140 °C (held for 1 min) at 15 °C/min, then to 300 °C (held for 20 min) at 3 °C/min. 1 μL of the solution was injected in splitless mode. A 30 m × 0.32 mm i.d. DB-5 (film thickness 0.25 μm) capillary column was used to separate compounds. The reference mixture Indiana STD provided by Indiana University, USA, which contained ten *n*-alkane homologues (nC_{12}, nC_{14}, nC_{16}, nC_{18}, nC_{20}, nC_{22}, nC_{25}, nC_{28}, nC_{30}, nC_{32}) was injected for identifying *n*-alkanes by comparison of retention times. The peak areas of *n*-alkanes were used to calculate relative abundance.

2.3.3. Hydrogen isotopic analysis

Hydrogen isotopic analyses were performed on a GC-TC-IRMS utilizing an HP-6890 GC and a GCC III connected to a Finnigan MAT Delta ^{Plus} XL isotope ratio mass spectrometer. Individual compounds separated by GC were pyrolysed by GCC III to convert organic H into H_2 at 1440 °C, and the H_2 was then introduced into the mass spectrometer for determination of isotopic composition. A 60 m × 0.32 mm i.d. HP-5 (film thickness 0.25 μm) capillary column was used. The GC temperature program for *n*-alkane separation ramped from 70 to 180 °C (held for 1 min) at 10 °C/min, then to 290 °C (held for 15 min) at 4 °C/min.

The analysis method followed Bi et al. (2005) and Jia et al. (2008). The H_3 factor for the mass spectrometer was determined daily by observing changes in the (mass-3)/(mass-2) ion-current ratio as the pressure of H_2 in the ion source varied. The instrument was tuned to ensure that the H_3 factor was always around 7. The reproducibility and accuracy of the hydrogen isotopic analyses were evaluated routinely using GC-IRMS reference materials (Indiana STD) with known δD values. During the measurement, laboratory standards were injected periodically (typically one standard injection per six sample analyses) to ensure that the mass spectrometer was stable. δD values of sample compounds were calculated relative to pulses of H_2 gas and were calibrated against the V-SMOW scale. During our measurements, the average and standard deviation of the measured δD values minused the observed for standard compounds is less than 3‰ and 4‰, respectively. All δD values reported in this study are the averages of triplicate analyses with the standard deviations of sample ranging from 0 to 6‰.

3. Results

3.1. Soil n-alkane abundance, distribution and δD value

n-Alkanes separated from topsoil of three transects range from nC_{25} to nC_{35}, with the most abundant being nC_{27}, nC_{29} and nC_{31}. There was a pronounced odd-over-even preference, as represented by the carbon preference index (CPI_{25-33}) of the *n*-alkanes, which varied between 2.9 and 42.9 with mean values of 7.2, 8.7 and 14.0 for Wuyi, Shennongjia and Tianshan, respectively (Fig. 3, Table S3). Significant differences were found in samples from between 3169 and 3489 m in the meadows of the Tianshan Mountains. Here, soils showed bimodal patterns of *n*-alkane distribution with a substantial nC_{21} contribution, especially in samples from 3169 m and 3272 m with the carbon number maximum (C_{max}) of nC_{21} (Fig. 3). Additionally, the sample from the highest site in the alpine cushion plant zone of the Tianshan Mountains was characterized by a much higher CPI_{25-33} value (42.9) and a C_{max} of nC_{33} (Fig. 3).

Individual *n*-alkane δD values of long chain *n*-alkanes nC_{27}, nC_{29}, nC_{31}, nC_{33} and nC_{21} are presented in Table S3. Due to the low concentrations, some δD values of nC_{31} and nC_{33} have not been determined. δD values of *n*-alkanes in individual samples showed no

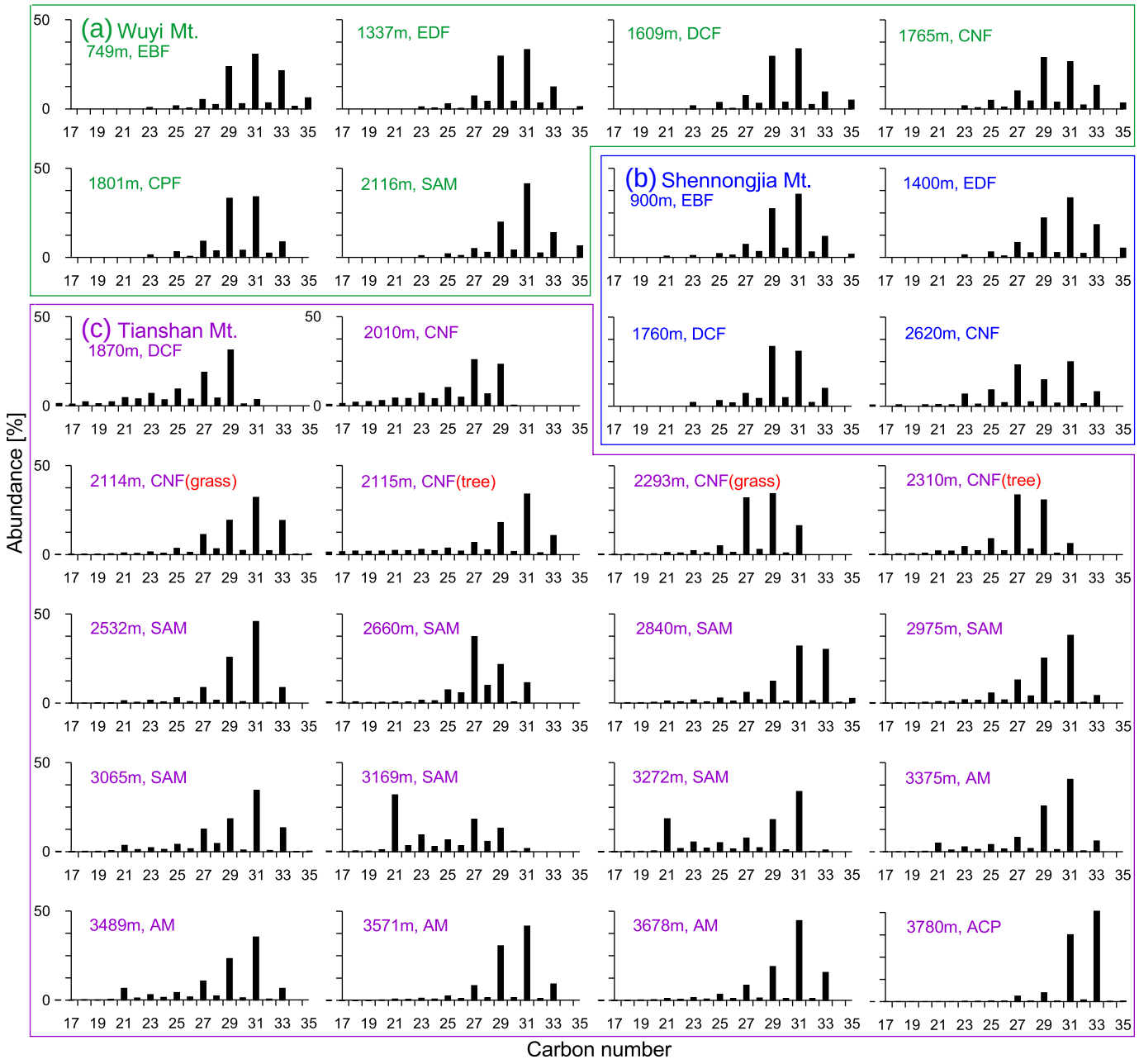

Fig. 3. Histogram of individual *n*-alkanes abundance from topsoil along Wuyi, Shennongjia and Tianshan transects. Samples with the same n-alkane distribution in the vegetation zone are not shown. The vegetation abbreviation is consistent with Fig. 2. Note that samples (2115 m and 2310 m) were taken from *Picea* forest understory, while samples (2114 m and 2293 m) were taken under mosaic-like meadow inlaid in the forest.

correlation with chain length, but did exhibit an isotopic variation within a small range (differences between maximum and minimum δD value for nC_{27}, nC_{29} and nC_{31} were 1.3~23.3‰, and standard deviations varied from 0.7 to 12.9‰). For all samples, δD values of long chain *n*-alkanes show strong inter-correlations (correlation coefficients 0.90 for nC_{27} and nC_{29}, 0.92 for nC_{29} and nC_{31}, 0.80 for nC_{31} and nC_{33}). δD values of *n*-alkanes co-varied with altitude (Fig. 4), with δD contents decreasing with altitude along the Wuyi, Shennongjia and Tianshan (below 3300 m) transects, while, conversely, increasing with altitude along the Tianshan transect above 3200 m.

3.2. δD values of precipitation

Precipitation samples were collected at Houxia station (2130 m, May 2003–July 2004) and Gaoshan station (3545 m, April 2003–July 2004) along the Tianshan transect. Annual and summer (June to August) weighted precipitation δD (δD_p) were −52.6‰ and −40.5‰ at Houxia, and −56.9‰ and −46.6‰ at Gaoshan. Very small δD_p lapse rates −0.30‰/100 m (annual) and −0.43‰/100 m (summer) between the two stations were observed. The isotopic signature of the precipitation at both Houxia and Gaoshan was characterized by a pronounced seasonal variation with high δD_p and low deuterium-excess (d) values in summer (rainy season), and low δD_p and high d values in winter. The local meteoric water lines (LMWL) and d values were $\delta D = 7.13\delta^{18}O + 0.40$, $d = 7.15$ (Houxia) and $\delta D = 6.99\delta^{18}O + 0.69$, $d = 8.54$ (Gaoshan).

For the Wuyi and Shennongjia transects, δD_p was calculated by the Online Isotope Precipitation Calculator (OIPC version 2.2, http://www.waterisotopes.org) using the GNIP database and interpolation algorithms described in Bowen and Revenaugh (2003) based on latitude, longitude and altitude of sample sites. There are 25 GNIP sites scattered in eastern

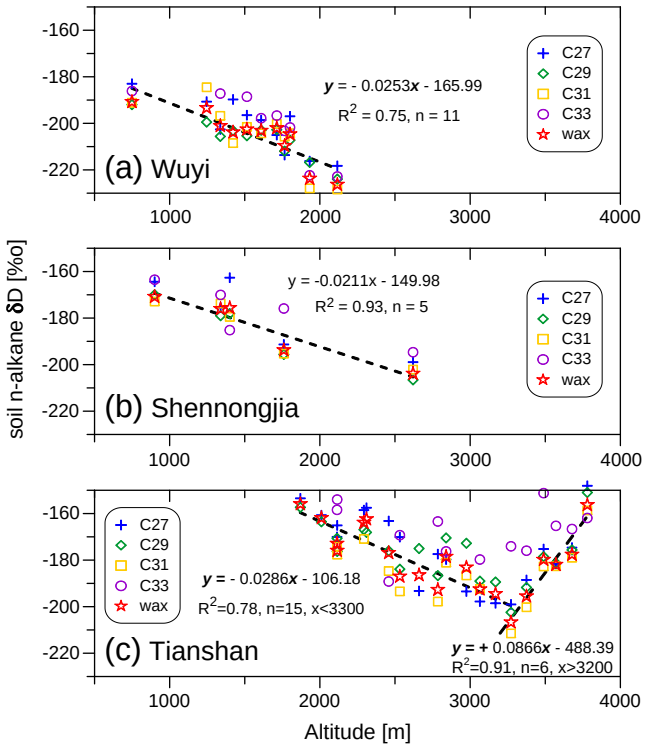

Fig. 4. Variations of δD values of *n*-alkanes derived from leaf wax in soils along altitudinal transects.

China (the monsoon area) with altitudes in the range 7–1892 m. We therefore believe that OIPC can provide constrained δD_p values only for low to mid altitude sample sites along the Wuyi and Shennongjia transects. Due to sparse GNIP sites along the Tianshan transect (Fig. 1) and complicated moisture sources in western China and central Asia, we only employ the measured δD_p rather than the predicted OIPC δD_p in this study.

The apparent (net) fractionation between leaf wax and precipitation ($\varepsilon_{wax\text{-}p}$) was calculated by:

$$\varepsilon_{wax-p} = (\delta D_{wax} + 1)/(\delta D_p + 1) - 1 \quad (1)$$

where δD_{wax} was the amount-weighted mean δD value of the leaf wax *n*-alkanes (nC_{27}, nC_{29} and nC_{31}). All available δD_p and $\varepsilon_{wax\text{-}p}$ values were listed in Table S3.

4. Discussion and implications

4.1. n-Alkane origins

The features of the long-chain *n*-alkane distribution (Fig. 3) and high CPI_{25-33} values (Table S3) reflect contributions from leaf waxes of terrestrial high plants to the soil organic matter (Cranwell, 1973; Eglinton and Hamilton, 1967; Lei et al., 2010). Soils from 3169 to 3489 m along the Tianshan transect demonstrate the bimodal pattern of mid-long length *n*-alkanes, especially in samples from 3169 m and 3272 m with a C_{max} of nC_{21} (Fig. 3). Previous studies indicate that mid-length *n*-alkanes (nC_{21}–nC_{25}) originated from submerged/floating-leaved plants (Ficken et al., 2000) or mosses (e.g., *Sphagnum*) (Baas et al., 2000). Aquatic macrophytes were absent from the Tianshan transect, because our sampling sites were on slopes and far away from water accumulation areas, while numerous mosses (e.g., *Bryum, Anornobryum, Pohlia, Sphagnum*) were present in the moist meadow zone intermixed with grasses and forbs. We infer that nC_{21} was derived from these mosses, reflecting changing environmental conditions with falling temperatures and increased soil moisture. In addition, the soil *n*-alkanes from the highest site in the alpine cushion plant zone (*Androsoe squarrosula, Sibbaldia tetrandra, Poa alpine* and lichen) of the Tianshan Mountains were characterized by a high CPI_{25-33} (42.9) and a C_{max} at nC_{33} (Fig. 3). The extended long-chain *n*-alkanes were considered as indicative of possible biosynthesis adaptations for physiological drought caused by freezing at high altitude (Shepherd and Griffiths, 2006).

4.2. n-Alkane δD gradients controlled by altitude effect

Soil *n*-alkanes in individual samples were derived from a variety of different plants, especially in the warm and moist Wuyi and Shennongjia Mountains with high biodiversity, yet the variation of δD values for nC_{27}, nC_{29} and nC_{31} fell into a small range (1.3~23.3‰) (Table S3, Fig. 4). Since δD_p and evaporative conditions at one particular site were constant, δD of water used by plants tended to be consistent. Therefore, the variation of *n*-alkane δD likely reflects different fractionation between source water and leaf wax among species or plant types (Hou et al., 2007b; Liu et al., 2006; Pedentchouk et al., 2008). Nevertheless, soil *n*-alkanes demonstrate relatively small δD variations, which suggests that mixed-origin *n*-alkanes, e.g. from soils and sediments, have reduced interspecies variations in apparent fractionation. Additionally, δD values of individual nC_{27}, nC_{29}, and nC_{31} alkanes along three altitudinal transects exhibited strong inter-correlations (correlation coefficient >0.90) and synchronous changes with altitude (Fig. 4), both of which imply a predominant factor relating to altitude for *n*-alkane δD changes. Thus, we use amount-weighted mean δD values of nC_{27}, nC_{29}, and nC_{31} as leaf wax δD (δD_{wax}) for the following discussion. δD_{wax} could integrate species-specific apparent fractionations (Jia et al., 2008), therefore it is more suitable for representing the general isotopic signal of local precipitation.

There were good linear relationships between δD_{wax} and altitude, and relatively similar isotopic lapse rates (R^2 values of 0.75, 0.93, 0.78, and lapse rates of −2.53, −2.11 and −2.86‰/100 m, respectively for Wuyi, Shennongjia and Tianshan below 3300 m). For the Tianshan Mountains above 3200 m, the relation was reversed, as will be discussed below. These δD_{wax} lapse rates fall into the reported δD_p lapse rate range −1~−4‰/100 m in mountainous areas (Araguás-Araguás et al., 2000; Clark and Fritz, 1997), and are approximately equal to the mean of −2.24‰/100 m estimated based on a $\delta^{18}O$ lapse rate of −0.28‰/100 m (Poage and Chamberlain, 2001) (multiplied by 8 in terms of the GMWL slope). Although the three altitudinal transects differ not only in terms of geographic location, climate background and moisture sources, but also in terms of climate gradients and along-transect vertical vegetation zones, the isotopic altitude effect of precipitation was found to control δD_{wax} altitudinal gradients in the mountains. This is because (1) the altitude effect is the common regulation and altitude is the primary factor controlling the distribution of precipitation isotopes in montane settings (Guan et al., 2009), and (2) precipitation is the source of leaf water, so its δD value determines the basic isotopic signature of leaf wax (Hou et al., 2008; Liu and Yang, 2008; Rao et al., 2009; Sachse et al., 2004, 2006). Our results from the three transects further confirm the ability of δD values of leaf wax-derived *n*-alkanes to act as a proxy for altitude.

4.3. The "inverse altitude effect" in the Tianshan Mountains

Above 3200 m along the Tianshan transect, δD values of nC_{27}, nC_{29} and nC_{31} increased rapidly with increasing altitude (Table S3, Fig. 4c). δD_{wax} became progressively enriched, from −206.7‰ to −156.3‰, at a rate of +8.66‰/100 m. The reasons responsible for the reversal of the δD_{wax} (or δD_{alkane}) gradient might be: (1) change of source water used by plants, (2) enhanced evaporation from soil and leaf surfaces due to aridity, (3) more positive taxon-specific $\varepsilon_{wax\text{-}p}$ in higher altitude areas, and (4) D-enrichment of precipitation at high altitudes. We discuss these factors in more detail below.

The source water used by plants in alpine meadow (AM) and alpine cushion (ACP), where the altitude gradient of δD_{wax} was reversed, would be surface soil water recharged by local precipitation. This is similar with the situation in subalpine meadow (SAM) which distributed at lower altitudes, because all sample sites were located on slopes that preserve shallow soil layers, and grasses/forbs in SAM, AM and ACP only have shallow roots (5–10 cm) and dense root hairs. There was no evidence to show that plants in AM and ACP use groundwater or deep soil water, both of which could finally result in the change of δD_{wax} (Krull et al., 2006). In addition, as shown in Figure 2, mean annual RH at the middle and high altitude sites was 58% and mean summer RH in the high altitude zone varied within 65–74%. There was no trend of decreased RH as altitude increases. On the other hand, although precipitation decreases slightly with increasing altitude in this section, the air temperature is quite low and decreases gradually. Consequently P/E (Precipitation/Evaporation) is likely to remain fairly constant. Therefore, the severely and progressively positive δD_{wax} cannot be interpreted by enhanced evaporative D-enrichment on soil and leaf surface because of relatively stable RH and P/E as altitude (Sachse et al., 2004, 2006; Smith and Freeman, 2006).

Studies based on individual plants and plant types indicate that $\varepsilon_{wax\text{-}p}$ is different among plant forms (e.g., tree/shrub/grass) (Hou et al., 2007b; Liu et al., 2006) and between angiosperms and gymnosperms (Pedentchouk et al., 2008). However, above 2400 m along the Tianshan transect, meadow was intermixed with grasses and herbs, and there were no gymnosperm plants and no obvious changes of plant form. We also find that, from 3065 m to 3489 m, δD of nC_{21} derived from moss (e.g., *Sphagnum*) clearly demonstrated co-variation with δD_{wax} (Table 3S, Fig. 6c), which suggest that the increase in δD_{wax} above 3200 m was not taxon related.

In summary, source water, evaporative condition and taxon-specific $\varepsilon_{wax\text{-}p}$ cannot account for the reversal δD_{wax} (or δD_{alkane}) gradient. Based on the δD_p of Houxia station (2130 m) and Gaoshan station (3545 m) and the average δD_{wax} values of the nearest two sample sites (2114 m and 2115 m in coniferous forest (CNF) at Houxia, and 3489 m and 3571 m in AM at Gaoshan), the calculated $\varepsilon_{wax\text{-}p}$ values were −128.6‰ and −131.5‰, respectively (Fig. 6c), both of which are consistent with the mean value of -133 ± 6‰ for terrestrial plants synthesized by Mügler et al. (2008). Note that the site at 2115 m was located in *Picea* forest understory and site 2114 m in meadow (*Festuca*, *Poa*, *Helictotrichon*) at the edge of the forest, and their $\varepsilon_{wax\text{-}p}$ values were not significantly different (−130.2‰ vs. −127.0‰). This indicates that $\varepsilon_{wax\text{-}p}$ in CNF characterized by mosaic-like forest-meadow and AM intermixed with grasses and forbs (*Carex, Kobresia, Polygonum, Poa alpina*) are similar. Moreover, due to the similarities in plant communities and life forms between meadow inlaid in CNF and SAM (*Kobresia, Artemisia, Festuca, Poa*), $\varepsilon_{wax\text{-}p}$ in SAM might be similar to that in the CNF meadow. Therefore, the terrestrial $\varepsilon_{wax\text{-}p}$ would be a constant, and −130‰ would be typical of each of CNF, SAM and AM (1900–3700 m) along the Tianshan transect.

Our study based on soil n-alkanes was restricted to determining the transpiration fractionation due to differences of leaf anatomy/morphology. However, we found that in the upper AM and the whole ACP, vegetation became lower and sparser, and leaf morphology changed significantly (e.g., leaf number increased, leaf thickness increased, leaf area decreased, leaf scale-shaped or needle-shaped, leaf cutinized or lignified, leaf surface hair appearance). These characteristics, which favor reduced evapotranspiration, reflect plant adaptations for physiological drought caused by freezing at high altitude (Wood, 2005), and possibly lead to more negative δD_{wax} (or $\varepsilon_{wax\text{-}p}$), rather than more positive. Other possible influences from fog, snowmelt and photosynthetic pathway also were discussed and excluded (see supplementary materials). Therefore, the "inverse altitude effect" of δD_{wax} is probably caused by isotopic enrichment of precipitation at high altitudes, as discussed in the following.

4.4. V-type variation of δD_{wax} in the Tianshan Mountains caused by the convergence of orographic upflow and westerlies

Two precipitation stations, Houxia (2130 m) and Gaoshan (3545 m), demonstrated much smaller isotopic lapse rates in summer (−0.43‰/100 m) and annual precipitation (−0.30‰/100 m) than those of reported mountainous δD_p lapse rates between −1 and −4‰/100 m (Araguás-Araguás et al., 2000; Clark and Fritz, 1997). However, for precipitation events occurring synchronously at both stations, the δD_p lapse rates were between −1.0 and −1.6‰/100 m at temperatures below 0 °C, whereas the altitude effect was absent or reduced at temperatures above 0 °C (Pang et al., Tellus-B, submitted). This suggests that under warm conditions, some hydrological processes induce precipitation within heavier isotopes in the alpine zone and disturb the altitude effect dominated by orographic uplift. Previous studies in this area have provided evidence for this possibility. For example, Zhang et al. (2003) reported a relatively small summer precipitation $\delta^{18}O$ lapse rate of −0.1‰/100 m between stations at 2336 m and 3545 m, and there was a reversal in the altitude effect in surface firn sampled from 3800 to 4000 m on the days with precipitation and on several subsequent days. Atmospheric circulation changes (Tian et al., 2007; Yao et al., 2009), sub-cloud evaporation (cloud-base evaporation from falling drops) (Froehlich et al., 2008; Gat, 2000), and secondary evaporation (re-evaporation of ground-level water) (Clark and Fritz, 1997) can lead to $D/^{18}O$ enrichment in precipitation. However, deuterium-excess and meteorological conditions at Gaoshan station imply that both sub-cloud evaporation and secondary evaporation do not significantly modify the isotopic composition of precipitation (Pang et al., Tellus-B, submitted).

The atmospheric circulation and precipitation processes are complicated in the Tianshan Mountains. As shown in Figure 2, there are two maximum precipitation zones along the transect: one at the entrance to a gap in the mountains (at Yingxiongqiao, ~1900 m) and the other in a glaciated area (at Daxigou, ~3500 m) (Han et al., 2004; Wang and Zhang, 1985). The former is attributed to the sharp orographic uplift, and the latter is thought to be due to the convergence of orographic upflow and katabatic flow on the glacier surface (Zhang and Lin, 1985). Meteorological analyses indicate that, in summer, precipitation occurs in the Tianshan Mountains and over extensive areas away from the mountains when cold fronts cross this area, and in the high mountain area when altostratus or nimbostratus move along trajectories of high-altitude westerlies; additionally, 76% of summer precipitation events begin earlier at high stations (the lag time of the lowest station relative to the highest is 4–5 hours (Wang and Zhang, 1985). In summary, high-altitude westerlies probably dominate the precipitation in the alpine zone of the Tianshan Mountains.

We speculate that the reversal of δD_p with altitude is caused by the increased contribution of isotope-enriched westerly moisture with altitude above a cutoff altitude (~3300 m). This has been suggested as one of the reasons for enriched precipitation on the northern Tibetan plateau relative to equivalent altitudes to the south as well as the reduced isotopic lapse rate on the northern plateau (Hren et al., 2009; Polissar et al., 2009; Yao et al., 2009). The westerly moisture was intercepted by high topography in the Tianshan Mountains, then its reduced contribution or/and the progressive rain-out process as altitude decreasing would result in the "inverse altitude effect" in the total precipitation. This conceptual model (westerly-dominated at high altitudes and orographic upflow-dominated at low-mid altitudes, see Fig. 5) fits climatological and meteorological observations, and also explains the small isotopic gradient between Houxia and Gaoshan stations. It further provides an explanation for a V-type precipitation isotope distribution along the Tianshan transect, and therefore could explain the V-type variation of δD_{wax} (Fig. 4).

The inverse altitude effect has been rarely reported. This is due to the absence of precipitation isotope data from high altitude areas. Additionally, the inverse altitude effect of snow and firn was attributed to post-deposition modification (e.g., Holdsworth et al.,

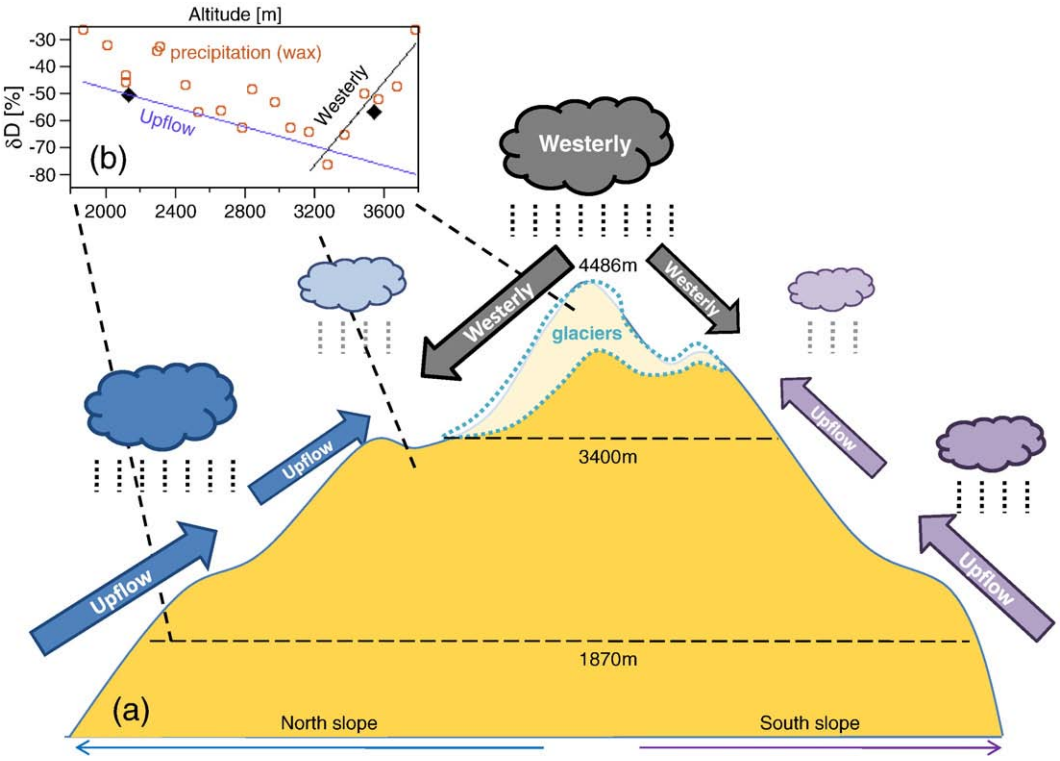

Fig. 5. Schematic diagram of atmospheric circulation in Tianshan Mt. and V-type distribution of δD_p predicted by the conceptual model. (a) Westerly dominates at high altitudes above the lower boundary of glaciers. Orographic upflow dominates at low-mid altitudes. They are assumed to converge at 3200~3400 m. (b) Black ◆ represents realistic δD_p at Houxia station (2130 m) and Gaoshan station (3545 m); red ○ presents δD_p estimated by δD_{wax} with $\varepsilon_{wax\text{-}p}$ value of −130‰. Blue solid line represents normal altitude effect of precipitation caused by the isolated upflow, which is predicted via simple Rayleigh model (Rowley and Garzione, 2007); black solid line represents inverse altitude effect of precipitation created by reduced contribution of D-enriched moisture or/and progressive rainout process of westerlies as altitude decreasing.

1991; Niewodniczanski et al., 1981; Zhang et al., 2003). However, the inverse altitude effect has been confirmed in the Canadian Rockies: positive $\delta^{18}O$-elevation gradients were found under strong westerly and northwesterly flows, when the Robertson Valley acts as a leeward slope; while more conventional negative gradients were found in the upslope flow, when easterly winds make the Robertson Valley a windward snow depositional environment (Moran et al., 2009). The impacts of atmospheric circulation and wind-slope geometry interactions on the altitude effect may therefore be larger than previously thought (Blisniuk and Stern, 2005; Galewsky, 2009; Yao et al., 2009). Understanding these factors could favor calibration of modeled/empirical isotope-altitude relationships. Moreover, these results imply that both topography and the pattern of atmospheric circulation in the past should be considered when interpreting changes of long-term δD and $\delta^{18}O$ records for elevation change.

4.5. Climate-specific $\varepsilon_{wax\text{-}p}$ and its response to altitude

All available $\varepsilon_{wax\text{-}p}$ data are listed in Table S3. Average values of $\varepsilon_{wax\text{-}p}$ in the Wuyi and Shennongjia Mountains are -154.2 ± 7.7‰ and -129.2 ± 7.3‰ respectively. As in the Tianshan Mountains, values of $\varepsilon_{wax\text{-}p}$ in CNF (−128.6‰) and in AM (−131.5‰) were determined and speculated to be constant at ~−130‰ along the transect (see section 4.3). The quite negative $\varepsilon_{wax\text{-}p}$ of Wuyi could be attributed to the extreme humid climate (RH > 80%, Fig. 2), the positive water balance (precipitation < evaporation and year-round precipitation (>1700 mm), Table S1) and the dense vegetation cover. These would lead to negligible D-enrichment (compared to other sites) in leaf water which could be explained alternately: relatively small evaporation occurs on soil and leaf surfaces due to high RH; non-fractionation transpiration dominates the water flux and so the soil water pools are not evaporatively D-enriched; a canopy effect creates a depleted δD value for water vapor that then exchanges with stomatal water leading to a more negative δD for leaf water. Though the Tianshan Mountains are located in relatively arid area, spring snowmelt and concentrated summer precipitation (Table S1) supply adequate water in the growing season (steppe is only distributed away from the mountains). Therefore, water availability in growing season in the Tianshan Mountains is similar with the moderately humid Shennongjia Mountains, which leads to their consistent $\varepsilon_{wax\text{-}p}$ values. Other studies also reveal the climate dependency of $\varepsilon_{wax\text{-}p}$. Values of $\varepsilon_{wax\text{-}p}$ from humid area, e.g., north–south lake sediment transects in Europe (-128 ± 12‰) (Sachse et al., 2004) and north–south surface soil transects in eastern China (−140 ~ −130‰) (Rao et al., 2009), are more negative than those in arid area, e.g., plants in southern California (-94 ± 21‰) (Feakins and Sessions, 2010). These results collectively imply that aridity or water stress in the growing season is the primary factor controlling $\varepsilon_{wax\text{-}p}$ — more arid, more positive $\varepsilon_{wax\text{-}p}$ values.

In addition, we found in the Shennongia and Tianshan Mountains and previous studies (Hou et al., 2008; Rao et al., 2009; Sachse et al., 2004) that despite a large range of environmental conditions and vegetation, soil/sediment $\varepsilon_{wax\text{-}p}$ still remains fairly constant, compared to variable $\varepsilon_{wax\text{-}p}$ in different plant types (Hou et al., 2007b; Liu et al., 2006) and individual plants (Sachse et al., 2009; Sessions, 2006). One of reasons would be that leaf waxes of soils/sediments, derived from multiple plants, integrate species-specific apparent fractionations (Jia et al., 2008). More importantly, under certain water availability conditions, the ecosystem can change its vegetation and plant physiology to adapt to environment change (Shepherd and Griffiths, 2006; Wood, 2005). As suggested by Hou et al. (2008), the influence of RH decrease on δD_{wax} across climatic gradients in the southern USA would be countered by the influence of vegetation change from woodland to grassland, which results in relative constant $\varepsilon_{wax\text{-}p}$. This eco-physiological adjustment might imply that soil/sediment $\varepsilon_{wax\text{-}p}$ is not affected significantly by mere vegetation

change and a climate-specific $\varepsilon_{wax\text{-}p}$ value can be used to reconstruct paleo-precipitation δD, or further for theoretical paleoaltimetry ($\delta D_{wax} - \delta D_{paleo\text{-}precipitaiton}$ — paleoaltitude) (e.g., Polissar et al., 2009). However, $\varepsilon_{wax\text{-}p}$ could be altered substantially when climate condition or water availability reaches a threshold and becomes a restrictive factor (Feakins and Sessions, 2010).

We therefore suggest climate-specific $\varepsilon_{wax\text{-}p}$ values: −150‰ for an extremely humid climate, −130‰ for a moderately humid climate and −100‰ for a typically arid climate. Meanwhile, we think that the "humid climate" is characterized by adequate summer precipitation (low water stress in the growing season) or no arid vegetation (steppe/shrub/desert). The climate-specific $\varepsilon_{wax\text{-}p}$ estimate (Feakins and Sessions, 2010; Hou et al., 2008; Sachse et al., 2004; and this study) is probably more feasible than the taxon-specific $\varepsilon_{wax\text{-}p}$ suggested by Liu and Yang (2008) and Pedentchouk et al. (2008). This is because (1) $\varepsilon_{wax\text{-}p}$ is not only modified by plant types, but also by climate parameters and complicated plant physiological changes and adaptations, both of which have not been fully understood; and (2) difficulties still exist in acquiring detailed paleo-flora data and in evaluating the contribution of variable plant species (or plant types) to sedimentary/paleosol organic matter.

Another important question for theoretical paleoaltimetry is how does $\varepsilon_{wax\text{-}p}$ change with altitude. Values of $\varepsilon_{wax\text{-}p}$ along the Tianshan transect were probably constant. However, though average $\varepsilon_{wax\text{-}p}$ for the low-mid altitude zones (ε_l) of the Wuyi and Shennongjia transects were constant at −151.0 ± 3.1‰ and −129.2 ± 0.9‰, respectively, but both of them (ε_h) become slightly more negative at high altitudes (Fig. 6). This amplified apparent fractionation could be attributed to the vegetation shift to grass/conifer (Hou et al., 2007b; Liu et al., 2006; Pedentchouk et al., 2008). And also as speculated by Jia et al.(2008), more negative $\varepsilon_{wax\text{-}p}$ values above 3500 m in the Gongga altitudinal transect are caused by the vegetation change from forest to meadow and shrub. Nevertheless, another explanation which turns to overestimate of δD_p values at high altitudes in the Wuyi, Shennongjia and Gongga transects is also reasonable. In our study, for the Wuyi and Shennongjia transects, δD_p are calculated by OIPC (based on GNIP dataset) in which implicit isotope lapse rate (−0.194‰/100 m for $\delta^{18}O$, Bowen and Revenaugh, 2003) is lower than that in mountains excluding GNIP dataset (−0.28‰/100 m for $\delta^{18}O$, Poage and Chamberlain, 2001). This weakness of OIPC, especially obvious at high elevations where lack of constrains of GNIP sites, would lead to the calculated δD_p values higher than the realistic δD_p at high altitudes, and pseudo more negative $\varepsilon_{wax\text{-}p}$. As for the Gongga transect, the situation is similar. Jia et al. (2008) used the GNIP Chengdu site (T = 289.25 K, RH = 82%) as the starting point of moisture source and modeled polynomial regression of the isotope-elevation relationship (T = 295 K, RH = 80%) by Rowley (2007), which also could result in the higher predicted δD_p because a steeper isotope lapse rate is expected in the colder area (Rowley, 2007; Rowley and Garzione, 2007).

In fact, the Rayleigh condensation process leads to the δD_p–altitude relationship deviates from linearity (the slope increases with altitude), especially in wet seasons/years (Gonfiantini et al., 2001). This means that realistic δD_p values at high altitudes would be more negative than those of linear prediction (e.g., OIPC). Therefore, observed more negative δD_{wax} in the humid Wuyi, Shennongjia and Gongga Mountains probably caused by more negative δD_p, rather than amplified $\varepsilon_{wax\text{-}p}$ by the vegetation change to grass/conifer. Therefore, soil/sediment $\varepsilon_{wax\text{-}p}$, which determined by regional climate, seems to do not change significantly with mere vegetation shift along altitudinal transects. But this speculation needs to be examined using realistic δD_p in the future work.

4.6. Empirical δD_{wax}-altitude relationship for paleoaltimetry

Another approach to paleoelevation reconstruction might be to directly employ an empirical δD_{wax}-altitude relationship. When the altitude effect is dominant, as in the Wuyi, Shennongjia, Tianshan (below 3200 m) and Gongga (Jia et al., 2008), altitudinal transects demonstrate good linear relationships between δD_{wax} and altitude ($R^2 > 0.74$) (Fig. 7). For the Wuyi and Gongga transects, quadratic functions ($R^2 > 0.81$) fit better than linear functions, which suggests, in the humid mountains, that δD_{wax} would tracks δD_p which follows quadratic variation with altitude controlled by the Rayleigh condensation process (Clark and Fritz, 1997; Gonfiantini et al., 2001). The mean δD_{wax} lapse rate of −2.27 ± 0.38‰/100 m (or −1‰/45 ± 8 m) indicates overall similar altitudinal gradients of δD_{wax}, although the four transects are located in different latitudes and vary in terms of moisture sources and environmental conditions. Since the altitudinal transect accounts for general patterns of climate, vegetation and landform evolution during mountain uplift, an empirical δD_{wax}–altitude relationship which integrates the influences of topography, climate and vegetation could be used to estimate paleoelevation change (not absolute paleoelevation) of mountains. However, since our empirical relationship was established in a relatively humid climate with vegetation including evergreen/deciduous/coniferous/mixed forest, meadow and cushion, the average gradient of −2.27 ± 0.38‰/100 m obtained here is only suitable for the uplift stages without an arid climate or steppe/shrub/desert ecosystem. Moreover, since moisture recycling (Hren et al., 2009; Yao et al., 2009) and amount effect (Gonfiantini et al., 2001; Peterse et al., 2009) could significantly alter the $\delta D/\delta^{18}O$ altitudinal gradient, our empirical relationship would need to be modified when used for regions affected by these hydrological processes.

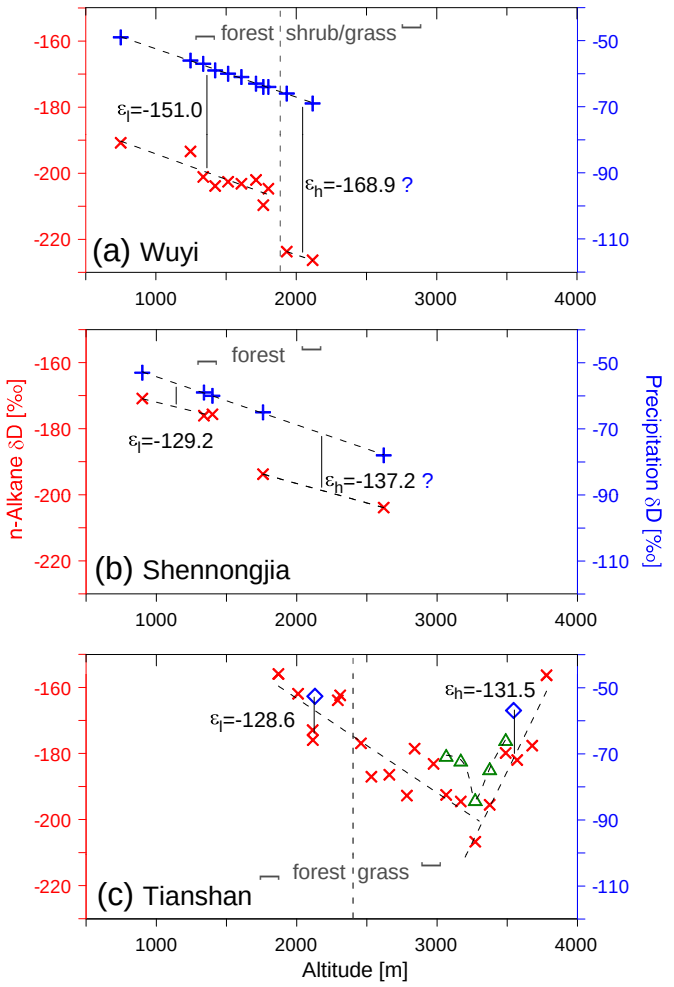

Fig. 6. Leaf wax δD (red ×), moss-derived nC_{21} δD (green △), precipitation δD (blue + for OIPC calculation; blue ◇ for realistic measurement), ε_l (the apparent fractionation between leaf wax and precipitation in low-mid altitude zone) and ε_h (in high altitude zone) along altitudinal transects.

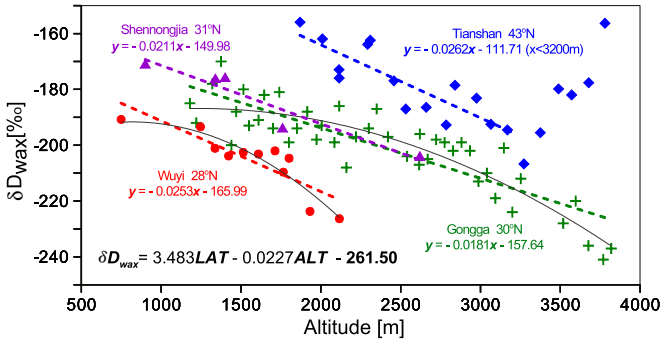

Fig. 7. Empirical δD_{wax}–altitude relationship synthesized from altitudinal transects in China. Results of the Gongga transect are from Jia et al. (2008).

As soil δD_{wax} of mountains in different latitudes have been presented in this study, the relationship between δD_{wax} and latitude can be assessed. Figure 8a shows that the intercept of the linear δD_{wax}–altitude formula (Fig. 7) correlates well with the mean latitude of the transect ($R^2 = 0.99$). Therefore, the relationship for δD_{wax}–latitude–altitude can be expressed by:

$$\delta D_{wax} = 3.483LAT - 0.0227ALT - 261.5 \quad (2)$$

The predicted δD_{wax} values from Eq. (2) fit well with the observations ($R^2 = 0.74$) (Fig. 8b). This function gives a preliminary spatial distribution pattern of δD_{wax} in present China and illustrates geographical controls of on δD_{wax}, The coefficient of ALT indicates the empirical altitude gradient of δD_{wax}, and the coefficient of LAT suggests more positive δD_{wax} values as latitude increasing (aridity enhanced). Additionally, Eq. (2) would provide an estimate of paleoaltitude as reference in terms of measured δD_{wax} and given paleolatitude in the montane settings of China when the past environmental pattern was strictly similar to the present. However, the coefficient of LAT and the constant of Eq. (2) would be much variable during the geological history and limit application in paleoaltimetry. But as the modern distribution pattern of δD_{wax}, Eq. (2) might to be refined when more δD_{wax}, altitude and latitude data are synthesized.

The theoretical paleoaltimetry (δD_{wax}–$\delta D_{paleo\text{-}precipitaiton}$–paleoaltitude) depends on clarification of $\varepsilon_{wax\text{-}p}$ response to altitude variation and establishment of the modeled/empirical δD_p–altitude relationship. For the undetermined $\varepsilon_{wax\text{-}p}$ as altitude, we have discussed in section 4.5. As for δD_p–altitude relationship, the current Rayleigh model is restricted to 35°N/S and to isolated orographic upflow (Rowley, 2007; Rowley and Garzione, 2007), while empirical isotope–altitude relationships need long term observations of precipitation, both of which present difficulties. By contrast, the δD_{wax} reflects the mean δD_p signal over a period of decades, and facilitates establishing local δD_{wax}–altitude relationships for empirical paleoaltimetry. We suggest to continue to investigate modern altitudinal transects of sediments/soils/plants, especially those covering dry or extreme cold climate and vegetation zones, in order to provide more $\varepsilon_{wax\text{-}p}$ data and abundant nearest relatives compatible for variable patterns of mountain uplift.

5. Conclusions

Leaf wax-derived *n*-alkane δD track altitudinal variations of precipitation δD along modern soil transects that span variable moisture sources, environmental conditions and vertical vegetation spectra, which confirm that δD_{wax} can act as a proxy for mountain altitude. The negative gradients in δD_{wax} along the Wuyi, Shennongjia and Tianshan altitudinal transects are overall similar. Together with the δD_{wax} gradient of the Gongga transect (Jia et al., 2008), an empirical δD_{wax}–

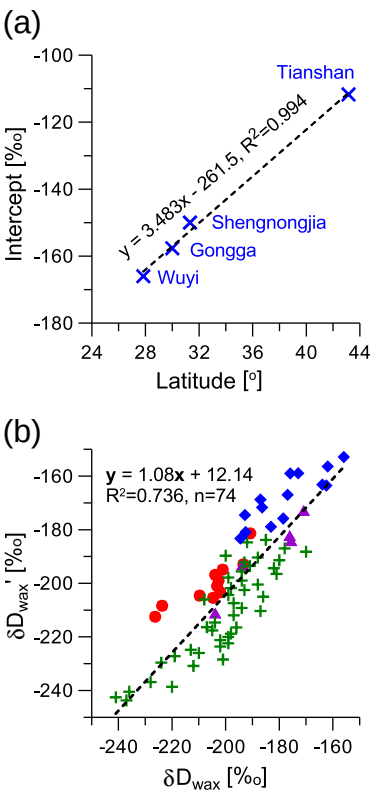

Fig. 8. (a) The relationship between intercept of linear δD_{wax}–altitude formula (Fig. 7) and mean latitude of each transect. (b) Comparison of realistic (δD_{wax}) δD values of leaf wax with predicted (δD_{wax}) calculated by $\delta D_{wax} = 3.483LAT - 0.0227ALT - 261.5$. Red ● (Wuyi), purple ▲(Shennongjia), green + (Gongga) and blue ◆ (Tianshan < 3200 m).

altitude relationship was established in which the average δD_{wax} lapse rate of -2.27 ± 0.38‰/100 m is suitable for estimating the relative uplift of mountains/plateau (paleoelevation change). The application of this empirical gradient would be restricted to stages of mountain uplift when (1) the climate was not arid, and dry steppe/shrub/desert was not dominant in the ecosystem, and (2) the atmospheric circulation was not substantially changed.

The empirical δD_{wax}–latitude–altitude formula was also determined, as: $\delta D_{wax} = 3.483LAT - 0.0227ALT - 261.5$. This provides the preliminary spatial distribution pattern of δD_{wax} in modern China and illustrates geographical controls on δD_{wax}, e.g., the coefficient of LAT suggests more positive δD_{wax} as latitude increasing (aridity enhanced).

The variations of δD values between nC$_{27}$, nC$_{29}$ and nC$_{31}$ in the individual soil sample fell into a small range, which suggest that soil/sediment δD_{wax} integrate species-specific apparent fractionations and reduce the deviation in n-alkanes δD values. Mean value of $\varepsilon_{wax\text{-}p}$ in the extreme humid Wuyi Mountains is quite negative (−154‰), compared to the humid Shennongjia (−129‰) and the arid (abundant summer precipitation) Tianshan Mountains (−130‰), which suggests aridity or water availability in the growing season is the primary factor controlling $\varepsilon_{wax\text{-}p}$. We therefore suggest climate-specific $\varepsilon_{wax\text{-}p}$ for reconstruction of precipitation δD and theoretical paleoaltimetry: −150‰ for an extremely humid climate, −130‰ for a moderately humid climate (or no water stress in the growing season) and −100‰ for a typically arid climate.

Along the Tianshan transects, values of $\varepsilon_{wax\text{-}p}$ are speculated to be constant with altitude; while along the Wuyi and Shennongjia transects, $\varepsilon_{wax\text{-}p}$ are also constant at the low-mid altitudes, but become slightly more negative at high altitudes which could be attributed to overestimates of δD_p by OIPC. Soil/sediment $\varepsilon_{wax\text{-}p}$, which determined by regional climate, seems to do not change significantly with mere vegetation change along altitudinal transects. However, the more negative δD_{wax} and $\varepsilon_{wax\text{-}p}$ are

also could be interpreted by the vegetation shift to grass/conifer (Jia et al., 2008; Liu and Yang, 2008; Pedentchouk et al., 2008), investigation of realistic water δD and physiological adaptations at high altitudes are therefore of continuing importance.

Evidence from observed precipitation δD, the V-type variation of δD_{wax} and meteorological analysis suggests that a reversal in the altitude effect of precipitation exists in the alpine zone of the Tianshan Mountains, which could be attributed to increased contribution of D-enriched westerly moisture with altitude above a cutoff altitude. This implies that the isotopic altitude effect is likely to be impacted, even reversed, by atmospheric circulations. Therefore, when interpreting long term isotope records for elevation change, the paleo-pattern of atmospheric circulation should be evaluated first.

Acknowledgments

This work was supported by the National Natural Science Foundation of China (Grant No. 40730208) and Knowledge Innovation Programs of the Chinese Academy of Sciences (Grant No. KZCX2-YW-Q09-03-02). We thank colleagues at Tianshan Glaciological Station, Chinese Academy of Sciences for sampling assistance; Chiling Yu for laboratory assistance; and Shiling Yang, Zihua Tang, Ling Gao, Lide Tian, Dabang Jiang, Yanlong Kong, Tianming Huang, Qinglong You and Klaus Froehlich for helpful communications or significant discussions. We also appreciate the constructive suggestions from two anonymous reviewers.

Appendix A. Supplementary data

Supplementary data to this article can be found online at doi:10.1016/j.epsl.2010.11.012.

References

Aizen, V.B., Aizen, E.M., Melack, J.M., Dozier, J., 1997. Climatic and hydrologic changes in the Tien Shan, Central Asia. J. Climate 10, 1393–1404.
Ambach, W., Eisner, H., Dansgaard, W., Moeller, J., 1968. The altitude effect on the isotopic composition of precipitation and glacier ice in the Alps. Tellus 20, 595–600.
Araguás-Araguás, L., Froehlich, K., Rozanski, K., 2000. Deuterium and oxygen-18 isotope composition of precipitation and atmospheric moisture. Hydrol. Process. 14, 1341–1355.
Baas, M., Pancost, R., van Geel, B., Damste, J.S.S., 2000. A comparative study of lipids in *Sphagnum* species. Org. Geochem. 31, 535–541.
Bi, X., Sheng, G., Liu, X., Li, C., Fu, J., 2005. Molecular and carbon and hydrogen isotopic composition of n-alkanes in plant leaf waxes. Org. Geochem. 36, 1405–1417.
Bishop, P., 2007. Long-term landscape evolution: linking tectonics and surface processes. Earth. Surf. Processes Landforms 32, 329–365.
Blisniuk, P.M., Stern, L.A., 2005. Stable isotope paleoaltimetry: a critical review. Am. J. Sci. 305, 1033–1074.
Bowen, G.J., Revenaugh, J., 2003. Interpolating the isotopic composition of modern meteoric precipitation. Water Resour. Res. 39, 1299.
Chikaraishi, Y., Naraoka, H., 2003. Compound-specific δD–δ^{13}C analyses of n-alkanes extracted from terrestrial and aquatic plants. Phytochemistry 63, 361–371.
Clark, I.D., Fritz, P., 1997. Environmental Isotopes in Hydrogeology. CRC Press LLC, New York.
Clark, M.K., 2007. The significance of paleotopography. Rev. Mineral. Geochem. 66, 1–21.
Cranwell, P.A., 1973. Chain-length distribution of n-alkanes from lake sediments in relation to post-glacial environmental change. Freshwater Biol. 3, 259–265.
Eglinton, G., Hamilton, R.J., 1967. Leaf epicuticular waxes. Science 156, 1322–1335.
Feakins, S.J., Sessions, A.L., 2010. Controls on the D/H ratios of plant leaf waxes in an arid ecosystem. Geochim. Cosmochim. Acta 74, 2128–2141.
Ficken, K.J., Li, B., Swain, D.L., Eglinton, G., 2000. An n-alkane proxy for the sedimentary input of submerged/floating freshwater aquatic macrophytes. Org. Geochem. 31, 745–749.
Forest, C.E., 2007. Paleoaltimetry: a review of thermodynamic methods. Rev. Mineral. Geochem. 66, 173–193.
Froehlich, K., Kralik, M., Papesch, W., Rank, D., Scheifinger, H., Stichler, W., 2008. Deuterium excess in precipitation of Alpine regions – moisture recycling. Isot. Environ. Health Stud. 44, 61–70.
Galewsky, J., 2009. Orographic precipitation isotopic ratios in stratified atmospheric flows: Implications for paleoelevation studies. Geology 37, 791–794.
Garzione, C.N., Quade, J., DeCelles, P.G., English, N.B., 2000. Predicting paleoelevation of Tibet and the Himalaya from δ^{18}O vs. altitude gradients in meteoric water across the Nepal Himalaya. Earth Planet. Sci. Lett. 183, 215–229.
Gat, J.R., 2000. Atmospheric water balance — the isotopic perspective. Hydrol. Process. 14, 1357–1369.
Gonfiantini, R., Roche, M.-A., Olivry, J.-C., Fontes, J.-C., Zuppi, G.M., 2001. The altitude effect on the isotopic composition of tropical rains. Chem. Geol. 181, 147–167.
Guan, H., Simmons, C.T., Love, A.J., 2009. Orographic controls on rain water isotope distribution in the Mount Lofty Ranges of South Australia. J. Hydrol. 374, 255–264.
Han, T.-d., Ding, Y.-j., Ye, B.-s., Xie, C.-w., 2004. Precipitation variations on the southern and northern slopes of the Tianger Range in Tianshan Mountains. J. Glaciol. Geocryol. 26, 761–766.
Holdsworth, G., Fogarasi, S., Krouse, H.R., 1991. Variation of the stable isotopes of water with altitude in the Saint Elias Mountains of Canada. J. Geophys. Res. 96, 7483–7494.
Hou, J., D'Andrea, W.J., MacDonald, D., Huang, Y., 2007a. Evidence for water use efficiency as an important factor in determining the δD values of tree leaf waxes. Org. Geochem. 38, 1251–1255.
Hou, J.Z., D'Andrea, W.J., Huang, Y.S., 2008. Can sedimentary leaf waxes record D/H ratios of continental precipitation? Field, model, and experimental assessments. Geochim. Cosmochim. Acta 72, 3503–3517.
Hou, J.Z., D'Andrea, W.J., MacDonald, D., Huang, Y.S., 2007b. Hydrogen isotopic variability in leaf waxes among terrestrial and aquatic plants around Blood Pond, Massachusetts (USA). Org. Geochem. 38, 977–984.
Hren, M.T., Bookhagen, B., Blisniuk, P.M., Booth, A.L., Chamberlain, C.P., 2009. δ^{18}O and δD of streamwaters across the Himalaya and Tibetan Plateau: implications for moisture sources and paleoelevation reconstructions. Earth Planet. Sci. Lett. 288, 20–32.
Hren, M.T., Pagani, M., Erwin, D.M., Brandon, M., 2010. Biomarker reconstruction of the early Eocene paleotopography and paleoclimate of the northern Sierra Nevada. Geology 38, 7–10.
Jia, G., Wei, K., Chen, F., Peng, P.a., 2008. Soil n-alkane δD vs. altitude gradients along Mount Gongga, China. Geochim. Cosmochim. Acta 72, 5165–5174.
Körner, C., 2007. The use of 'altitude' in ecological research. Trends Ecol. Evol. 22, 569–574.
Krull, E., Sachse, D., Mugler, I., Thiele, A., Gleixner, G., 2006. Compound-specific δ^{13}C and delta δD analyses of plant and soil organic matter: a preliminary assessment of the effects of vegetation change on ecosystem hydrology. Soil Biol. Biochem. 38, 3211–3221.
Kutzbach, J.E., Guetter, P.J., Ruddiman, W.F., Prell, W.L., 1989. Sensitivity of climate to Late Cenozoic Uplift in Southern Asia and the American West: numerical experiments. J. Geophys. Res. 94, 18393–18407.
Lei, G., Zhang, H., Chang, F., Pu, Y., Zhu, Y., Yang, M., Zhang, W., 2010. Biomarkers of modern plants and soils from Xinglong Mountain in the transitional area between the Tibetan and Loess Plateaus. Quatern. Int. 218, 143–150.
Li, Z., Manfred, D., 2002. Species richness of vascular plants along the climatic gradient of mountain Shennongjia in Central China. J. Shanghai Univ. 6, 265–268.
Liu, W., Yang, H., 2008. Multiple controls for the variability of hydrogen isotopic compositions in higher plant n-alkanes from modern ecosystems. Global Change Biol. 14, 2166–2177.
Liu, W.G., Yang, H., Li, L.W., 2006. Hydrogen isotopic compositions of n-alkanes from terrestrial plants correlate with their ecological life forms. Oecologia 150, 330–338.
Mügler, I., Sachse, D., Werner, M., Xu, B.Q., Wu, G.J., Yao, T.D., Gleixner, G., 2008. Effect of lake evaporation on δD values of lacustrine n-alkanes: a comparison of Nam Co (Tibetan Plateau) and Holzmaar (Germany). Org. Geochem. 39, 711–729.
Meyer, H.W., 2007. A review of paleotemperature—Lapse rate methods for estimating paleoelevation from fossil floras. Rev. Mineral. Geochem. 66, 155–171.
Molnar, P., Boos, W.R., Battisti, D.S., 2010. Orographic controls on climate and Paleoclimate of Asia: thermal and mechanical roles for the Tibetan Plateau. Annu. Rev. Earth Planet. Sci. 38, 77–102.
Moran, T.A., Marshall, S.J., Evans, E.C., Sinclair, K.E., 2009. Altitudinal gradients of stable isotopes in lee–slope precipitation in the Canadian Rocky Mountains. Arct. Antarct. Alpine Res. 39, 455–467.
Mulch, A., Chamberlain, C.P., 2007. Stable isotope paleoaltimetry in orogenic belts — the silicate record in surface and crustal geological archives. Rev. Mineral. Geochem. 66, 89–118.
Niewodniczanski, J., Grabczak, J., Baranski, L., Rzepka, J., 1981. The altitude effect on the isotopic composition of snow in high mountains. J. Glaciol. 97, 99–111.
Pedentchouk, N., Sumner, W., Tipple, B., Pagani, M., 2008. δ^{13}C and δD compositions of n-alkanes from modern angiosperms and conifers: an experimental set up in central Washington State, USA. Org. Geochem. 39, 1066–1071.
Peterse, F., van der Meer, M.T.J., Schouten, S., Jia, G., Ossebaar, J., Blokker, J., Sinninghe Damsté, J.S., 2009. Assessment of soil n-alkane δD and branched tetraether membrane lipid distributions as tools for paleoelevation reconstruction. Biogeosciences 6, 2799–2807.
Poage, M.A., Chamberlain, C.P., 2001. Empirical relationships between elevation and the stable isotope composition of precipitation and surface waters: considerations for studies of paleoelevation change. Am. J. Sci. 301, 1–15.
Polissar, P.J., Freeman, K.H., Rowley, D.B., McInerney, F.A., Currie, B.S., 2009. Paleoaltimetry of the Tibetan Plateau from D/H ratios of lipid biomarkers. Earth Planet. Sci. Lett. 287, 64–76.
Quade, J., Garzione, C., Eiler, J., 2007. Paleoelevation reconstruction using pedogenic carbonates. Rev. Mineral. Geochem. 66, 53–87.
Rao, Z., Zhu, Z., Jia, G., Henderson, A.C.G., Xue, Q., Wang, S., 2009. Compound specific δD values of long chain n-alkanes derived from terrestrial higher plants are indicative of the δD of meteoric waters: evidence from surface soils in eastern China. Org. Geochem. 40, 922–930.
Rowley, D.B., 2007. Stable isotope-based paleoaltimetry: theory and validation. Rev. Mineral. Geochem. 66, 23–52.

Rowley, D.B., Garzione, C.N., 2007. Stable isotope-based paleoaltimetry. Annu. Rev. Earth Planet. Sci. 35, 463–508.
Rowley, D.B., Pierrehumbert, R.T., Currie, B.S., 2001. A new approach to stable isotope-based paleoaltimetry: implications for paleoaltimetry and paleohypsometry of the High Himalaya since the Late Miocene. Earth Planet. Sci. Lett. 188, 253–268.
Ruddiman, W., Raymo, M., Prell, W., Kutzbach, J., 1997. The Uplift-Climate Connection: A Synthesis. Tectonic uplift and climate change: 471˚C11.
Sachse, D., Kahmen, A., Gleixner, G., 2009. Significant seasonal variation in the hydrogen isotopic composition of leaf-wax lipids for two deciduous tree ecosystems (*Fagus sylvativa* and *Acer pseudoplatanus*). Org. Geochem. 40, 732–742.
Sachse, D., Radke, J., Gleixner, G., 2004. Hydrogen isotope ratios of recent lacustrine sedimentary n-alkanes record modern climate variability. Geochim. Cosmochim. Acta 68, 4877–4889.
Sachse, D., Radke, J., Gleixner, G., 2006. δD values of individual n-alkanes from terrestrial plants along a climatic gradient — implications for the sedimentary biomarker record. Org. Geochem. 37, 469–483.
Sahagian, D., Proussevitch, A., 2007. Paleoelevation measurement on the basis of vesicular basalts. Rev. Mineral. Geochem. 66, 195–213.
Schimmelmann, A., Sessions, A.L., Mastalerz, M., 2006. Hydrogen isotopic (D/H) composition of organic matter during diagenesis and thermal maturation. Annu. Rev. Earth Planet. Sci. 34, 501–533.
Sessions, A.L., 2006. Seasonal changes in D/H fractionation accompanying lipid biosynthesis in Spartina alterniflora. Geochim. Cosmochim. Acta 70, 2153–2162.
Sessions, A.L., Sylva, S.P., Summons, R.E., Hayes, J.M., 2004. Isotopic exchange of carbon-bound hydrogen over geologic timescales. Geochim. Cosmochim. Acta 68, 1545–1559.
Shepherd, T., Griffiths, D.W., 2006. The effects of stress on plant cuticular waxes. New Phytol. 171, 469–499.
Smith, F.A., Freeman, K.H., 2006. Influence of physiology and climate on δD of leaf wax n-alkanes from C3 and C4 grasses. Geochim. Cosmochim. Acta 70, 1172–1187.
Teixell, A., Bertotti, G., de Lamotte, D.F., Charroud, M., 2009. The geology of vertical movements of the lithosphere: an overview. Tectonophysics 475, 1–8.
Tian, L.D., Yao, T.D., MacClune, K., White, J.W.C., Schilla, A., Vaughn, B., Vachon, R., Ichiyanagi, K., 2007. Stable isotopic variations in west China: a consideration of moisture sources. Journal of Geophysical Research-Atmospheres 112.
Wang, D., Zhang, P., 1985. On the valley climate of Urumqi River in the Tianshan Mountains. J. Glaciol. Geocryol. 7, 239–248.
Wood, A., 2005. Eco-Physiological Adaptations to Limited Water Environments. In: Jenks, M.A., Hasegawa, P.M. (Eds.), Plant abiotic stress. Wiley-Blackwell, pp. 1–13.
Yang, H., Huang, Y., 2003. Preservation of lipid hydrogen isotope ratios in Miocene lacustrine sediments and plant fossils at Clarkia, northern Idaho, USA. Org. Geochem. 34, 413–423.
Yao, T., Zhou, H., Yang, X., 2009. Indian monsoon influences altitude effect of $\delta^{18}O$ in precipitation/river water on the Tibetan Plateau, Chinese. Sci. Bull. 54, 2724–2731.
Zhang, B., Wu, H., Xiao, F., Xu, J., Zhu, Y., 2009. Integration of data on Chinese mountains into a digital altitudinal belt system. Mt. Res. Dev. 26, 163–171.
Zhang, J., Lin, Z., 1985. Climate of China. Shanghai Scientific & Technical Publishers, Shanghai.
Zhang, X., Yao, T., Liu, J., 2003. Oxygen-18 in different waters in Urumqi River Basin. J. Geog. Sci. 13, 438–446.